Dynamic optical arbitrary waveform generation and measurement

Ryan P. Scott,* Nicolas K. Fontaine, Jonathan P. Heritage, and S. J. B. Yoo

Department of Electrical and Computer Engineering, University of California, Davis, One Shields Ave., Davis, California, 95616, USA
**rpscott@ucdavis.edu*

Abstract: We introduce a dynamic optical arbitrary waveform generation (OAWG) technique that produces bandwidth scalable, continuous waveforms of near perfect fidelity. Additionally, OAWG's complement, real-time arbitrary optical waveform measurement (OAWM) is discussed. These approaches utilize gigahertz-bandwidth electronics to generate, or measure, truly arbitrary and dynamic optical waveforms scalable to terahertz bandwidths and infinite record lengths. We describe the theory, algorithms and enabling technologies necessary to calculate and produce a set of spectral modulations that create continuous, high-fidelity waveforms in the presence of spectral filtering from multiplexers.

OCIS codes: (320.0320) Ultrafast optics; (320.5540) Pulse shaping; (320.7100) Ultrafast measurements.

References and links

1. K. Takiguchi, K. Okamoto, T. Kominato, H. Takahashi, and T. Shibata, "Flexible pulse waveform generation using silica-waveguide-based spectrum synthesis circuit," Electron. Lett. **40**(9), 537–538 (2004).
2. Z. Jiang, D. E. Leaird, and A. M. Weiner, "Line-by-line pulse shaping control for optical arbitrary waveform generation," Opt. Express **13**(25), 10431–10439 (2005).
3. P. J. Delfyett, S. Gee, C. Myoung-Taek, H. Izadpanah, L. Wangkuen, S. Ozharar, F. Quinlan, and T. Yilmaz, "Optical frequency combs from semiconductor lasers and applications in ultrawideband signal processing and communications," J. Lightwave Technol. **24**(7), 2701–2719 (2006).
4. N. K. Fontaine, R. P. Scott, J. Cao, A. Karalar, W. Jiang, K. Okamoto, J. P. Heritage, B. H. Kolner, and S. J. Yoo, "32 Phase X 32 amplitude optical arbitrary waveform generation," Opt. Lett. **32**(7), 865–867 (2007).
5. R. P. Scott, N. K. Fontaine, J. Cao, K. Okamoto, B. H. Kolner, J. P. Heritage, and S. J. B. Yoo, "High-fidelity line-by-line optical waveform generation and complete characterization using FROG," Opt. Express **15**(16), 9977–9988 (2007).
6. Z. Jiang, C.-B. Huang, D. E. Leaird, and A. M. Weiner, "Optical arbitrary waveform processing of more than 100 spectral comb lines," Nat. Photonics **1**(8), 463–467 (2007).
7. R. P. Scott, N. K. Fontaine, C. Yang, D. J. Geisler, K. Okamoto, J. P. Heritage, and S. J. B. Yoo, "Rapid updating of optical arbitrary waveforms via time-domain multiplexing," Opt. Lett. **33**(10), 1068–1070 (2008).
8. N. K. Fontaine, R. P. Scott, L. Zhou, F. Soares, J. P. Heritage, and S. J. B. Yoo, "Real-time full-field arbitrary optical waveform measurement," Nat. Photonics **4**(4), 248–254 (2010).
9. N. K. Fontaine, "Optical arbitrary waveform generation and measurement," Ph.D. dissertation (University of California, Davis, 2010).
10. N. K. Fontaine, D. J. Geisler, R. P. Scott, T. He, J. P. Heritage, and S. J. B. Yoo, "Demonstration of high-fidelity dynamic optical arbitrary waveform generation," Opt. Express (submitted for publication).
11. N. K. Fontaine, R. P. Scott, C. Yang, D. J. Geisler, J. P. Heritage, K. Okamoto, and S. J. B. Yoo, "Compact 10 GHz loopback arrayed-waveguide grating for high-fidelity optical arbitrary waveform generation," Opt. Lett. **33**(15), 1714–1716 (2008).
12. F. M. Soares, J. H. Baek, N. K. Fontaine, X. Zhou, Y. Wang, R. P. Scott, J. P. Heritage, C. Junesand, S. Lourdudoss, K. Y. Liou, R. A. Hamm, W. Wang, B. Patel, S. Vatanapradit, L. A. Gruezke, W. T. Tsang, and S. J. B. Yoo, "Monolithically integrated InP wafer-scale 100-channel × 10-GHz AWG and Michelson interferometers for 1-THz-bandwidth optical arbitrary waveform generation," in *Optical Fiber Communication Conference*, OSA Technical Digest (CD) (Optical Society of America, 2010), Paper OThS1.
13. T. He, N. K. Fontaine, R. P. Scott, D. J. Geisler, J. P. Heritage, and S. J. B. Yoo, "Optical arbitrary waveform generation based packet generation and all-optical separation for optical-label switching," IEEE Photon. Technol. Lett. **22**(10), 715–717 (2010).
14. D. J. Geisler, N. K. Fontaine, T. He, R. P. Scott, L. Paraschis, J. P. Heritage, and S. J. Yoo, "Modulation-format agile, reconfigurable Tb/s transmitter based on optical arbitrary waveform generation," Opt. Express **17**(18), 15911–15925 (2009).

#131467 - $15.00 USD Received 12 Jul 2010; revised 6 Aug 2010; accepted 7 Aug 2010; published 17 Aug 2010

15. C.-B. Huang, D. E. Leaird, and A. M. Weiner, "Time-multiplexed photonically enabled radio-frequency arbitrary waveform generation with 100 ps transitions," Opt. Lett. **32**(22), 3242–3244 (2007).
16. J. T. Willits, A. M. Weiner, and S. T. Cundiff, "Theory of rapid-update line-by-line pulse shaping," Opt. Express **16**(1), 315–327 (2008).
17. R. G. Lyons, *Understanding Digital Signal Processing,* 2nd ed. (Prentice Hall PTR, Upper Saddle River, 2004).
18. R. Trebino, *Frequency-Resolved Optical Gating: The Measurement of Ultrashort Laser Pulses* (Kluwer Academic, Boston, 2000).
19. M. K. Smit, and C. Van Dam, "PHASAR-based WDM-devices: Principles, design and applications," IEEE J. Sel. Top. Quantum Electron. **2**(2), 236–250 (1996).
20. K. Okamoto, "Recent progress of integrated optics planar lightwave circuits," Opt. Quantum Electron. **31**(2), 107–129 (1999).
21. N. K. Fontaine, Y. Jie, J. Wei, D. J. Geisler, K. Okamoto, H. Ray, and S. Yoo, "Active arrayed-waveguide grating with amplitude and phase control for arbitrary filter generation and high-order dispersion compensation," in *34th European Conference on Optical Communication (ECOC 2008)*, Technical Digest (CD) (IEEE, 2008), 1–2. *http://dx.doi.org/10.1109/ECOC.2008.4729152*

1. Introduction

Most recently, the availability of phase-stable, gigahertz-rate optical frequency combs and high-resolution pulse shapers has facilitated demonstrations of truly arbitrary optical waveforms. This work is typically referred to as line-by-line pulse shaping or optical arbitrary waveform generation (OAWG) [1–7]. Existing OAWG work has been essentially limited to repetitive, albeit complex, waveforms that cannot be directly modified at gigahertz rates. Therefore, we refer to line-by-line shaping as static-OAWG since the repetitive arbitrary optical waveforms are generated via Fourier synthesis (i.e., the amplitude and phase of each comb line is set to equal the spectrum, or Fourier transform, of the desired temporal waveform) and the modulations are very slow when compared to the frequency spacing of the input optical frequency comb (OFC).

This paper introduces *dynamic-OAWG*, a technique to achieve high-fidelity, continuous generation of arbitrary optical waveforms of scalable bandwidth using optical frequency combs, spectral multiplexers, and an array of modulators. We present theory and simulations to demonstrate that there are actually numerous sets of comb line modulations that generate the same waveform. By example, we show how our dynamic-OAWG algorithm produces optimum modulations for high-fidelity continuous waveforms, even in the presence of multiplexer filtering. Additionally, there are discussions of enabling technologies for dynamic-OAWG including electro-optical modulators and spectral multiplexers. The final section of the paper describes an analogous real-time waveform characterization technique called optical arbitrary waveform measurement (OAWM) [8]. Because of their close symmetry, the theoretical treatment of dynamic-OAWG and OAWM is nearly interchangeable. However, to avoid confusion, this paper develops the theory in relation to OAWG. Additionally, we concentrate on implementations that use integrated optical device technologies due to the availability of high-speed modulators in lithium niobate, indium phosphide (InP), or silicon platforms, as well as the significant advantages in stability, size, weight, and cost associated with integrated solutions. Further examples and simulations of dynamic-OAWG and OAWM are available in [9] and an experimental demonstration of dynamic-OAWG is presented in [10].

1.1. A brief review of static-OAWG

Figure 1 shows the general concept of static-OAWG in which a stable input OFC is spectrally demultiplexed so that each comb line is at a separate spatial location (e.g., waveguide). Then, a modulator adjusts the relative spectral amplitude and phase of each comb line to a target value. This set of constant amplitude and phase shifts are the static-OAWG modulations. Finally, the output multiplexer coherently combines the different frequencies onto a single output. This combination of demultiplexer, modulators, and multiplexer is often referred to as a waveform shaper. Since the modulations are static, the waveform shaper is essentially a highly-configurable optical filter which is able to spectrally resolve the OFC.

Because the static-OAWG waveform shaper is a filter, its input and output are both frequency combs with a maximum bandwidth equal to the input OFC. However, since each

#131467 - $15.00 USD Received 12 Jul 2010; revised 6 Aug 2010; accepted 7 Aug 2010; published 17 Aug 2010

comb line is individually adjusted, the output waveforms can completely fill the OFC period. To create stable, high-fidelity waveforms, it is absolutely necessary to maintain the coherence, or phase relationship, of the comb lines through the waveform shaper. This is easy to accomplish in integrated optical devices such as silica planar lightwave circuits (PLCs) [1,11] or monolithic InP devices [12] since the waveguides cover a small physical area and are on a common substrate. Alternatively, well-designed free-space waveform shapers [2,6] can also create stable waveforms since most environmental effects are common-mode fluctuations on the shaped OFC. Therefore, there is no change in the relative amplitude and phase of the comb lines and very little distortion of the waveform envelope.

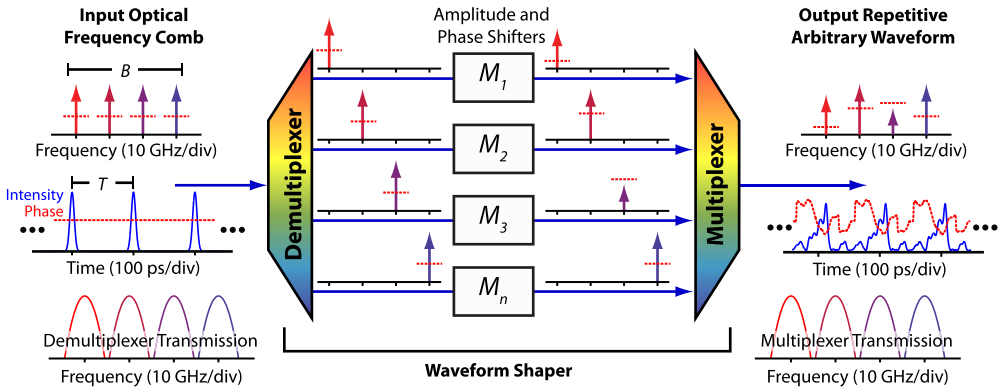

Fig. 1. An illustration which shows a typical static-OAWG arrangement for waveform shaping via Fourier synthesis. M_1–M_n represent modulators that adjust the relative amplitude and phase of the comb lines. Spectral power is represented by arrow height and phase by the vertical position of the dashed line.

1.2. Dynamically updating static-OAWG

In spite of its repetitive nature, many interesting static-OAWG applications are demonstrated in the literature [3,13–15]. Yet, the most impressive and pivotal applications will not be demonstrated until it is possible to continuously generate optical waveforms over intervals that greatly exceed the OFC period. To that end, a first approach is to instantaneously switch the static-OAWG modulations each comb period. This technique is referred to as rapid-update static-OAWG. As pointed out by Willits et al. [16], the synthesized waveforms will not update instantaneously because the output spectral multiplexer filters the modulations on each comb line. Alternatively, one must wait for the modulations to settle after passing through the multiplexer. Since the waveforms take some time to update, continuous high-fidelity waveform generation is impossible when using a spectral multiplexer.

Conceptually, rapid-update static-OAWG temporally slices a long waveform (i.e., many OFC periods) into subwaveforms of duration equal to the OFC period. Then for each subwaveform, the static-OAWG modulations are determined via Fourier synthesis as if that subwaveform were repeating. However, there are three crucial problems with using rapid-update static-OAWG modulations. (1) Excessive modulation bandwidth is required since the rapid-update static-OAWG modulations must instantaneously switch when transitioning from one subwaveform to the next. (2) Only a lossy $N \times 1$ star coupler can be used at the output of the waveform shaper since a standard spectral multiplexer would filter the modulations, thereby distorting the waveform. (3) Subwaveforms have excessive bandwidth since the process of temporally slicing the long arbitrary waveform with bandwidth, B, into subwaveforms introduces instantaneous transitions at the edges. Therefore, the static-OAWG representation of each subwaveform is not necessarily bandlimited to B. Section 5.3 provides details and simulations that clearly demonstrate the three problems listed above. All of the disadvantages of rapid-update static-OAWG are avoided by approaching the dynamic

#131467 - $15.00 USD Received 12 Jul 2010; revised 6 Aug 2010; accepted 7 Aug 2010; published 17 Aug 2010

generation of waveforms from a new, and perhaps broader, perspective that we call dynamic-OAWG. The following sections describe the concept in detail, including enabling technologies, algorithms for calculating the spectral modulations, and supporting simulations.

2. The dynamic-OAWG concept

Here we present a general outline of dynamic-OAWG with further details presented in later sections. Figure 2 shows a conceptual picture of dynamic-OAWG and to understand it, we must set aside the static-OAWG methods and analyze the target waveform from a different perspective. Instead of defining the target waveform over a single OFC period at a time, the target waveform is analyzed over much longer time periods (temporal slices). In other words, the spectra of long waveforms are created instead of the waveform's spectrum for only one OFC period. Although the long waveforms have complex spectra that are continuous, we show that it is possible to divide up the spectrum into manageable parts (spectral slices) that are produced in parallel and coherently summed to create the target spectrum.

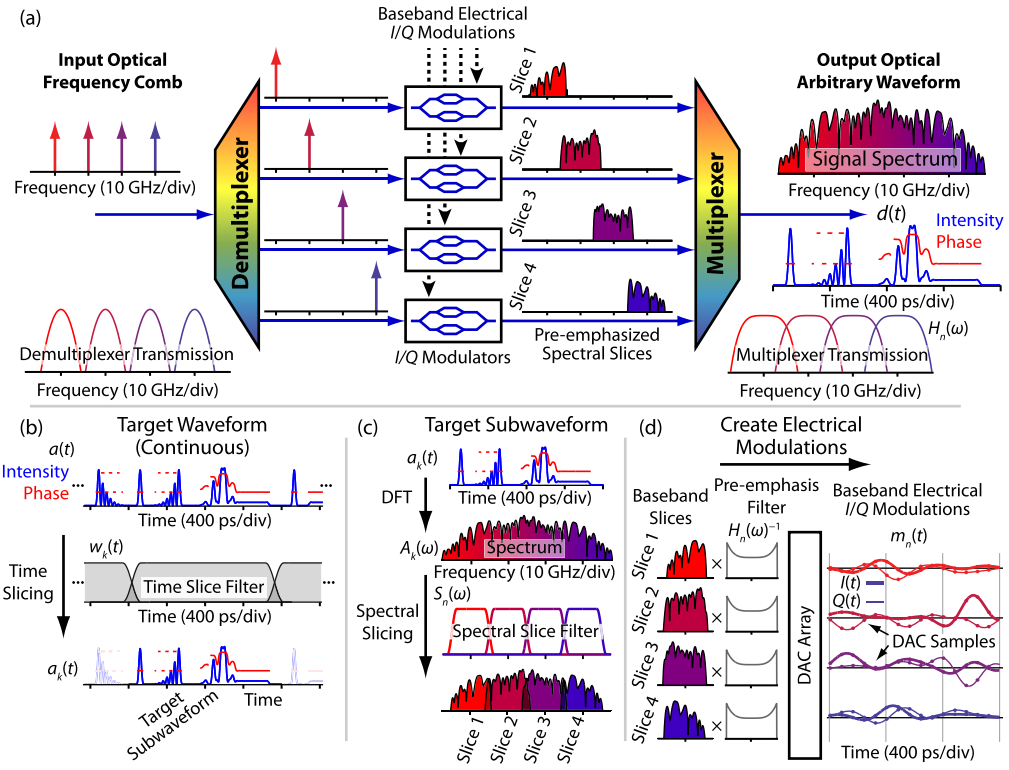

Fig. 2. Overview of dynamic-OAWG. (a) Each line of an OFC is simultaneously and independently modulated to create the desired spectral slices. A gapless multiplexer coherently combines the spectral slices to create the desired waveform. (b) In DSP, the target waveform is temporally sliced into subwaveforms. (c) The subwaveforms are spectrally sliced. (d) Baseband electrical *I/Q* modulations are calculated and produced. DAC: digital-to-analog converter.

Figure 2(a) shows how the OFC is modulated into the target waveform. After demultiplexing to separate waveguides, each comb line is independently optically modulated using the baseband *I/Q* signals of Fig. 2(d). A signal multiplexer, $H(\omega)$, coherently combines the modulated lines (now spectral slices) into a single contiguous complex spectrum that exactly matches the target waveform. To determine the required electrical *I/Q* modulations, the target waveform is processed by a digital signal processor (DSP) in the following manner: the continuous target waveform [Fig. 2(b)] is temporally sliced into long subwaveforms (i.e., many OFC periods). The complex spectrum of each subwaveform is calculated [Fig. 2(c)] and

#131467 - $15.00 USD Received 12 Jul 2010; revised 6 Aug 2010; accepted 7 Aug 2010; published 17 Aug 2010

subsequently spectrally sliced using a set of spectral slice filters. Here, the spectral slice filters are gapless and their center-to-center spacing is equal to the OFC spacing. The modulations necessary to create each complex spectral slice are pre-emphasized for the multiplexer [Fig. 2(d)] before a digital-to-analog converter (DAC) array produces each of the electrical signals. The output sample rate must be equivalent to, or greater than, the slice bandwidth (i.e., Nyquist rate for quadrature sampling [17]). The temporal modulations of adjacent subwaveforms are stitched together and when done correctly, the resulting continuous modulations maintain their fidelity.

A fundamental concept in dynamic-OAWG is that multiple sets of modulations can generate the same waveform. This is because a set of modulations can produce overlapping spectral slices (i.e., non-orthogonal basis functions). The only requirement is that the coherent summation of all the spectral slices, including the multiplexer filtering, equals the target waveform [see Eq. (3)]. This is unlike static-OAWG techniques, where a set of dc modulations produces non-overlapping or orthogonal spectral slices (i.e., individual comb lines). In this case, only one set of dc modulations will generate exactly one unique waveform.

An arbitrary waveform's shortest temporal feature is inversely proportional to its bandwidth B. In dynamic-OAWG, B is equal to the number of spectral slices multiplied by the slice spacing. Thus, to achieve a desired waveform bandwidth or temporal resolution, there is a tradeoff between the number of spectral slices (more complex optics for more slices) and the slice bandwidth (more complex electronics for broader slice bandwidth) which must be optimized. The 10 GHz slice spacing indicated in Fig. 2 falls in the frequency range where optical demultiplexers, modulators, and DACs overlap, while simultaneously maximizing the generation bandwidth and minimizing the system complexity. For instance, the fastest commercial electronic DACs have 5–10 GHz of analog bandwidth and set an upper limit on the slice spacing. Higher resolution AWGs require larger areas and set the lower limit of the slice spacing. By studying the dynamic-OAWG algorithm it is possible to optimize OAWG device designs and determine the best tradeoffs between the various system parameters.

There are many characteristics to consider when generating a waveform, including its overall complexity, minimum temporal feature size, total record length, spectral resolution, bandwidth, and fidelity (dynamic range). A waveform's complexity is commonly characterized by its time-bandwidth product (i.e., the waveform duration multiplied by its optical bandwidth) [18]. Therefore, dynamic-OAWG's capability to continuously generate arbitrary waveforms means that it can create infinitely complex waveforms for a given optical bandwidth. Continuous generation also implies that dynamic-OAWG has no theoretical limit on the spectral resolution of generated waveforms. This is a major improvement over static-OAWG where the spectral resolution is limited to the resolution of the waveform shaper. In dynamic-OAWG, the achievable fidelity is determined by the stability of the OFC and the performance of the components within the waveform shaper (e.g., isolation of the demultiplexer, effective number of bits (ENOB) of the DAC, extinction ratio of the modulators, etc.).

3. Enabling technologies for dynamic-OAWG

3.1. Optical modulation

In general, optical modulation maps a driving signal onto an optical carrier and generates both positive and negative frequencies with respect to the carrier. For simplicity, we concentrate on electro-optical modulation; however optical-optical modulation is just as valid. There are numerous types of modulator structures, however only structures capable of producing all possible complex optical waveforms within a specified information bandwidth are of interest for dynamic-OAWG. Additionally, a practical modulator structure needs to be spectrally efficient at mapping the modulation information to the optical domain (i.e., the information bandwidth equals the optical bandwidth). As an example of a complicated waveform, Fig. 3(a) depicts the temporal amplitude and phase of a band-limited arbitrary waveform, $a(t)$, as a 400-ps-long trajectory of a vector which traverses all four quadratures within the real-

#131467 - $15.00 USD Received 12 Jul 2010; revised 6 Aug 2010; accepted 7 Aug 2010; published 17 Aug 2010

imaginary plane. This trajectory could represent the modulation necessary to produce a single spectral slice such as that shown in Fig. 2(a). Figure 3(b) shows the waveform's complex spectrum which has a total optical bandwidth of 10 GHz.

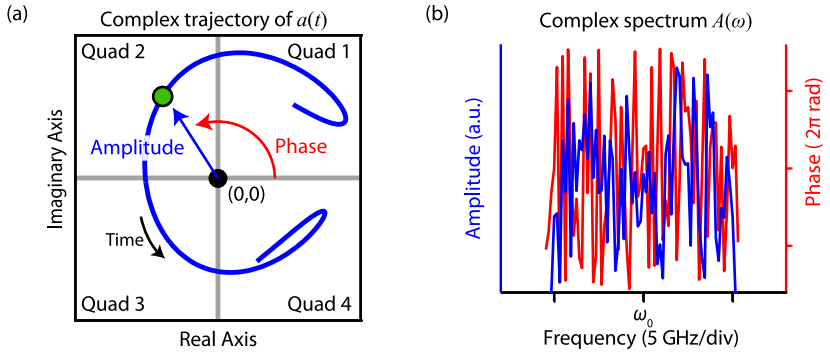

Fig. 3. (a) A complex modulation example showing the amplitude and phase of a 400-ps-long trajectory across the real-imaginary plane. (b) Corresponding calculated complex optical spectrum of the trajectory. ω_0 is the optical carrier.

Figure 4 shows two different electro-optic modulator structures that provide access to all four-quadratures of the real-imaginary plane by using two independent scalar modulation signals. Figure 4(a) shows the polar modulation structure, an amplitude and phase modulator in series. It is an instinctive and common structure where the amplitude and phase of the optical carrier are independently modulated in the time domain. Figure 4(b) is a calculation of the equivalent amplitude and phase modulation necessary to reproduce the trajectory shown in Fig. 3(a). Recreating the trajectory requires either an instantaneous phase jump of 2π rad or an extremely large peak phase modulation capability (endless phase modulation) to avoid the phase jumps. Analyzing the modulation signals' electrical power spectra, displayed in Fig. 4(c), shows that are they are not bandlimited to 10 GHz. This is true even for the amplitude modulation which does not contain any instantaneous jumps. Thus, it is easy to see that the polar modulation structure is impractical and bandwidth inefficient at recreating an arbitrary trajectory across the four field quadratures.

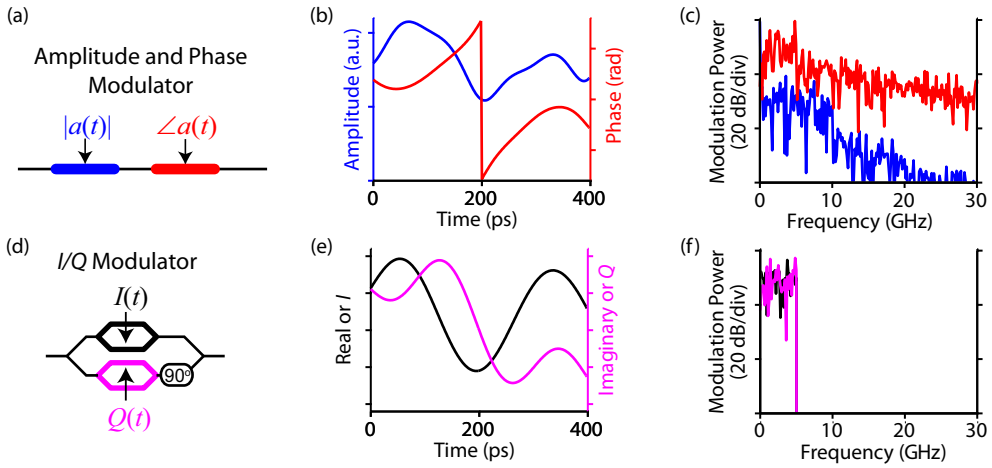

Fig. 4. Two different optical vector modulator structures. (a) Amplitude and phase modulators. (b) Electrical signals required to recreate the trajectory in Fig. 3(a). (c) Electrical power spectra of signals in (b). (d) *I/Q* modulator. (e) Electrical signals required to recreate the trajectory in Fig. 3(a). (f) Electrical power spectra of signals in (e).

#131467 - $15.00 USD Received 12 Jul 2010; revised 6 Aug 2010; accepted 7 Aug 2010; published 17 Aug 2010

Figure 4(d) shows an increasingly familiar modulation structure, known as the in-phase/quadrature-phase (*I/Q*) modulator. It consists of nested push-pull Mach-Zehnder modulators (MZM) with their outputs combined 90° out of phase. One MZM manipulates the *I*-field while the other MZM manipulates the *Q*-field and since the *I/Q* modulator uses direct mapping of the scalar signals to the optical field (when operating in its linear regime); it is a spectrally efficient structure. Quadrature modulation has the added advantage that the required electrical bandwidth per MZM necessary to recreate a particular trajectory is one-half of the total optical bandwidth of that trajectory [17]. Thus, we use a slightly more complicated structure to minimize the required electrical signal complexity and bandwidth. Figure 4(e) shows the *I/Q* modulation signals required to reproduce the trajectory of Fig. 3(a). Figure 4(f) presents the calculated modulation signals' electrical power spectra where both *I* and *Q* are each bandlimited to 5 GHz. Another, often overlooked, advantage of the *I/Q* modulator is that it is possible to trade increased insertion loss for a reduced drive voltage requirement. When using *I/Q* modulation, reaching all possible phase values does not require a peak phase modulation of ± π rad. Instead, you can restrict the maximum achievable amplitude, and still cover a full circle (centered on the origin) in the real-imaginary plane. Thus it is possible to reproduce an amplitude scaled version of any trajectory.

3.2. Spectral multiplexers

Specialized spectral multiplexers with optimized transmission are enablers for high-fidelity dynamic-OAWG. From Fig. 2(a), the dynamic-OAWG demultiplexer must isolate individual comb lines. However, a practical dynamic-OAWG implementation necessitates that the multiplexer can combine the modulated signals without excessive filtering of energy at the edges of the passbands. Ideally, the combined transmission function of the multiplexer/demultiplexer should provide very strong rejection of adjacent comb lines so that the final waveform fidelity is not impacted. OAWG implementations which use free-space optics typically use diffraction gratings in a 4–*f* pulse shaper configuration [2] to act as the spectral multiplexer and demultiplexer. However, arrayed-waveguide gratings (AWG) are the spectral multiplexer/demultiplexer of choice in an integrated optic implementation [19,20] because they are compact and offer easy control over the passband shape. For demonstration of passband control, Fig. 5 depicts an 'arbitrary filter' version of the AWG [21]. The amplitude and phase shifters on the waveguide array can adapt the filter response.

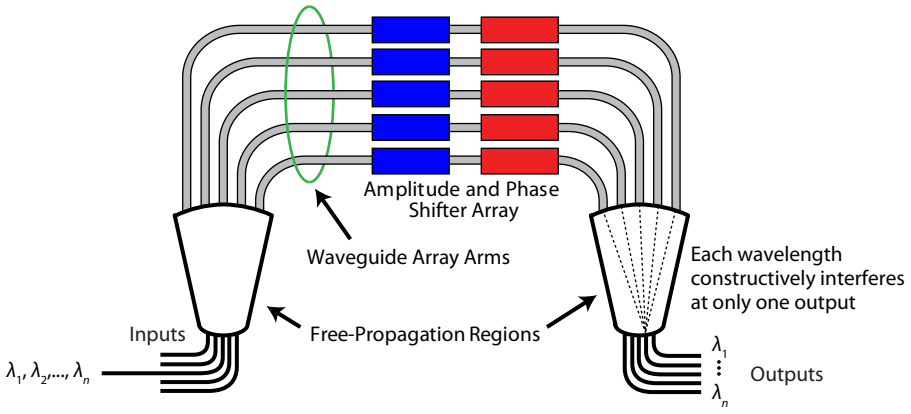

Fig. 5. Illustration of an arbitrary filter arrayed-waveguide grating (AWG).

Figure 6 shows transmission measurement data from an arbitrary filter AWG which was shaped into several multiplexers with different filter (passband) shapes that facilitate dynamic-OAWG. This arbitrary filter AWG has 16 arms with tunable amplitude and phase transmission of each arm so that it acts as a 16-tap finite impulse response (FIR) filter. The six outputs have a frequency spacing of 100 GHz, but designs with channel spacing from 5 GHz to 200 GHz are also possible. Figure 6(a) shows transmission measurement data for the

#131467 - $15.00 USD Received 12 Jul 2010; revised 6 Aug 2010; accepted 7 Aug 2010; published 17 Aug 2010

arbitrary filter AWG when it is configured as a spectral multiplexer with narrow passbands. The filter's high adjacent-channel isolation is ideal for separating individual comb lines from an OFC. This filter shape is achieved by placing a linear phase across the array arms. Figure 6(b) shows a transmission measurement when the arbitrary filter AWG is configured with a flat-top passband shape. Since it is flat across the majority of the passband, but still has relatively high isolation of adjacent channels, it would work well as both an input demultiplexer and an output multiplexer (i.e., little energy is lost at the edges of passband). This particular shape is created by applying a sinc function across the waveguide array arms (i.e., amplitude and phase modulators are both used). Figure 6(c) shows a measurement of the arbitrary filter when it is operating as a 'defocused' AWG which results when quadratic phase is applied across the array arms. Alternatively, the AWG free propagation region design could have the inputs closer to the output waveguides so that they are in a defocused position. Since the passbands of the defocused multiplexer are very broad and strongly overlapping (passbands overlap at −2 dB points), it combines modulated signals without significant filtering of the energy. However, it has some quadratic spectral phase across the passband which must be included when calculating the spectral slice modulations.

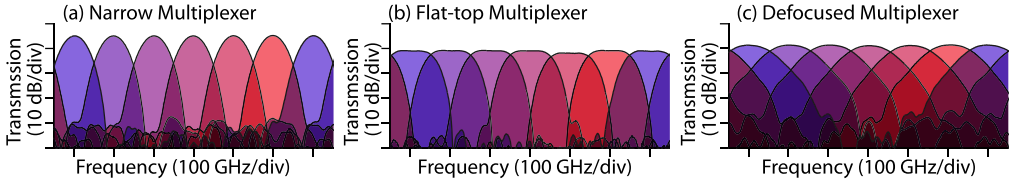

Fig. 6. Transmission measurements of an arbitrary filter AWG when configured for three different passband shapes. (a) A low-loss, narrow-bandwidth, and high adjacent-channel isolation passband. (b) A gapless, flat-top passband. (c) A gapless, broad-bandwidth passband (defocused AWG).

A dynamic-OAWG device can be built using arbitrary filter AWGs for the demultiplexer and multiplexer. However, it is much simpler to just design standard narrow passbands for the demultiplexer and a defocused AWG for the multiplexer. In conjunction with the dynamic OAWG algorithm/theory described in Section 5, the performance of the defocused multiplexer is comparable to the flat-top multiplexer.

4. Mathematical framework for dynamic-OAWG

Before delving into the details of dynamic-OAWG, we present the basic mathematical elements that are used in the rest of this work. First, the temporal envelope of an optical frequency comb $a_R(t)$ is defined as

$$a_R(t) = \sum_{n=-\infty}^{+\infty} R_n \exp(\mathrm{j}n\Delta\omega t), \tag{1}$$

where R_n is a coefficient that defines the amplitude and phase of the n-th comb line and $\Delta\omega$ is the comb line spacing in the frequency domain. (i.e., $\Delta\omega = 2\pi/T$ where T is the OFC period). Equation (1) is in the form of an inverse discrete Fourier transform (IDFT). Therefore, the waveform $a_R(t)$'s shape is controlled by the R_n coefficients and it is repetitive in nature with a period T. Figure 7 shows how two different sets of R_n produce two unique waveforms. For generality, the frequency axis is scaled to the OFC repetition rate, $1/T$, and the time axis is scaled to the OFC period, T.

Ultimately, the dynamic-OAWG device applies time varying modulations, $m_n(t)$, to each comb line with the intent to produce a waveform $a_m(t)$ that is continuous. We can define a frequency comb with modulated lines as

$$a_m(t) = \sum_{n=-\infty}^{+\infty} m_n(t) R_n \exp(\mathrm{j}n\Delta\omega t). \tag{2}$$

#131467 - $15.00 USD Received 12 Jul 2010; revised 6 Aug 2010; accepted 7 Aug 2010; published 17 Aug 2010

As mentioned previously, there are many sets of $m_n(t)$ that can produce $a_m(t)$ with bandwidth B. At a minimum, a set of $m_n(t)$ must be able to broaden each comb line to create a continuous spectrum. For example, the set of modulations that are the most electrically bandwidth efficient occur when the modulation bandwidth is equal to the comb spacing. The most inefficient (demanding) set of electrical modulations occur when one comb line is modulated at the full bandwidth B and all other comb lines are off. A reasonable compromise between the two extreme cases takes place when the spectral slices partially overlap at their edges. The spectral-slice OAWG algorithm discussed in Section 5.2 provides a rigorous method to find many sets of modulations. By optimizing the parameters of the algorithm, the required bandwidths of the modulations and the computation time or latency are minimized.

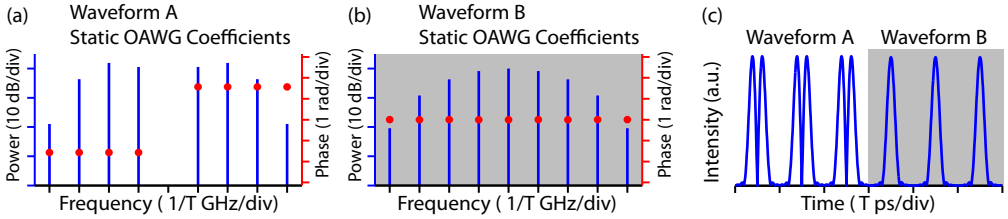

Fig. 7. Examples of two frequency combs with different sets of R_n. (a) Spectral coefficients for a zero-π pulse and (b) a transform-limited pulse. (c) Corresponding time domain plots where shading indicates coefficients used.

Not all sets of modulations satisfying Eq. (2) are compatible with a particular choice of spectral multiplexers. That is, due to the filtering properties of the multiplexers; the modulations are distorted so much that it is not possible to combine them into the desired target waveform. To determine if a set of modulations produce the target waveform, $a(t)$, it is sufficient to check if the line-by-line sum of the product of the spectral slices and spectral filtering equals the target waveform's spectrum, $A(\omega)$. Mathematically, this is

$$A(\omega) = \sum_{n=-\infty}^{+\infty} R_n M_n(\omega - n\Delta\omega) H_n(\omega), \tag{3}$$

where the individual spectral modulations, $M_n(\omega)$, are the Fourier transform (FT) of the temporal modulations, $m_n(t)$, and $H_n(\omega)$ is the complex transmission function for the n-th comb line through the multiplexer. When this equation is satisfied, the modulations will produce the target waveform. Such modulations are termed compatible with the spectral multiplexer. Correcting distortions due to the multiplexer filtering requires pre-emphasis of the modulations which is explained in more detail in the following section.

5. The dynamic-OAWG algorithm

The dynamic-OAWG algorithm is designed to continuously compute a set of bandlimited modulations, $m_n(t)$, that when applied to a demultiplexed frequency comb, will exactly synthesize a continuous arbitrary optical waveform, $a(t)$, with bandwidth B. As Fig. 2(b)–2(d) illustrates, the algorithm provides continuous waveform generation in four steps: (1) temporally slice $a(t)$ into subwaveforms $a_k(t)$, (2) spectrally slice the k-th subwaveform's spectrum into n slices, each corresponding to the n-th line of the OFC, (3) determine the exact modulations needed for each subwaveform's spectral slices using the spectral-slice OAWG (SS-OAWG) algorithm, and (4) temporally sum the n-th spectral slice modulations for the subwaveforms. This last step provides continuous modulations for each spectral slice and the temporal slicing also permits computational parallelization of the algorithm.

A major component of the dynamic-OAWG algorithm is the SS-OAWG algorithm which finds a set of modulations, $M_n(\omega)$, that are a solution to Eq. (3). Since it involves computing the DFT of $a(t)$, the SS-OAWG algorithm is restricted to periodic waveforms and prohibits continuous generation (i.e., $a(t)$ must be specified for its entire duration). To overcome this restriction, the dynamic-OAWG algorithm finds $m_n(t)$ to generate $a(t)$ in a series of smaller

#131467 - $15.00 USD Received 12 Jul 2010; revised 6 Aug 2010; accepted 7 Aug 2010; published 17 Aug 2010

subwaveforms $a_k(t)$. When the time-slicing is performed optimally, these computed modulations are the same as those provided by the infinite length SS-OAWG modulations.

5.1. Temporal slicing and spectral slicing

Figure 8(a) and 8(b) shows two temporal slice filter examples and Fig. 8(c) and 8(d) shows two spectral slice filter examples. The slice filters are a mathematical construct to break the waveform or its spectrum into time-limited or bandwidth-limited portions so that it is possible to compute modulations for continuous waveforms in a bandwidth scalable fashion. Although it is possible to create temporal slice filters with various complex shapes, we use two simple filters to demonstrate general principles and point out some issues with regard to dynamic-OAWG. Figure 8(a) shows a simple rectangular filter and Fig. 8(b) shows raised-cosine temporal filter with a shape equivalent to $\beta = 1/2$ (i.e., 50% excess width). For simplicity, the temporal slice filters have a uniform shape [i.e., $w_k(t) = w(t)$] with a center-to-center spacing of T_S. Therefore, when the temporal slicing is applied to the continuous waveform, it generates k subwaveforms, $a_k(t) = a(t)w(t - kT_S)$ each with a duration T_L. The summation of a set of slice filters must equal unity so that the summation across all $a_k(t)$ is $a(t)$. Temporal slice filters can overlap and this provides significant flexibility with the subwaveforms shape to produce compatible modulations.

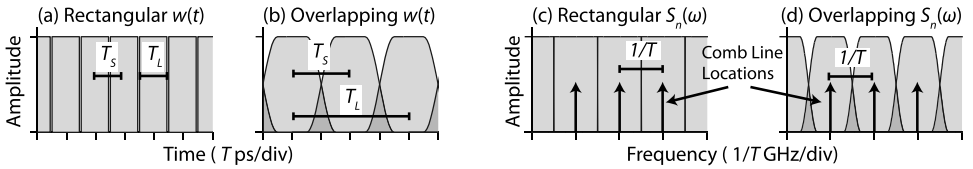

Fig. 8. Examples of slice filters in the (a,b) time and (c,d) frequency domains. Temporal slice filters have flexible spacing, T_S. Spectral slice filters are at the OFC repetition rate ($1/T$).

In a set of spectral slice filters which have a shape, $S_n(\omega)$, the n-th slice filter is associated with the n-th line of the OFC. The spectral slice filters are assumed identical in shape and each is centered on a comb line [see Fig. 8(c) and 8(d)]. It is the application of slice filters in both the time and frequency domains that makes many solutions to Eq. (2) possible.

5.2. The spectral-slice OAWG algorithm and examples

The SS-OAWG algorithm finds a set of comb line modulations that produce a periodic waveform's spectrum by solving Eq. (3) for a given multiplexer [Fig. 2(c) and 2(d)]. Here, we temporarily allow that the subwaveform, $a_k(t)$, of duration T_L is repetitive (with period T_L) so that the modulations can be calculated. First, the subwaveform's spectrum, $A_k(\omega)$, is computed using a DFT. Then the n-th spectral modulation of the k-th subwaveform is

$$M_{k,n}(\omega - n\Delta\omega) = \left[A_k(\omega)/R_n\right]\left[S_n(\omega)/H_n(\omega)\right]. \quad (4)$$

The second term forms the corrected slice filter $B_n(\omega) = S_n(\omega)/H_n(\omega)$ which includes pre-emphasis for the spectral multiplexer [i.e., $H_n(\omega)^{-1}$]. Substituting Eq. (4) into Eq. (3) yields

$$A_k(\omega) = \sum_{n=-\infty}^{+\infty} A_k(\omega)S_n(\omega), \quad (5)$$

which holds true when the summation across a set of only the spectral slice filters is unity. The IDFT of the spectral modulations, $M_{k,n}(\omega)$, are the temporal modulations, $m_{k,n}(t)$, necessary to generate a periodic version of $a_k(t)$.

Each set of spectral slice filters produces a different set of modulations compatible with the multiplexer as long as $B_n(\omega)$ is finite where $S_n(\omega)$ is non-zero. Additionally, the impulse response of the corrected slice filter, $b_n(t)$, predicts the shape of the temporal modulations. For example, using the rectangular spectral slice filter in Fig. 8(c) produces modulations bandlimited to the comb spacing. Because of the rectangular spectral shape, these modulations

#131467 - $15.00 USD Received 12 Jul 2010; revised 6 Aug 2010; accepted 7 Aug 2010; published 17 Aug 2010

will have a sinc-like ringing in the time domain. Using the overlapping slice filter of Fig. 8(d) reduces the ringing in the time domain and even reduces the amount of pre-emphasis needed at the expense of slightly more bandwidth. Optimizing $B_n(\omega)$ is critical, since excessive amounts of pre-emphasis will increase optical losses through the OAWG device and reduce the effective dynamic range. Additionally, it will set limits on the temporal-slice spacing for high-fidelity continuous waveform generation.

Figure 9 illustrates how the SS-OAWG algorithm computes modulations when applied to two extreme waveform cases: (a) a waveform with duration equal to the OFC spacing (i.e., $T_L = T$) and (b) a waveform with a relatively long duration. All simulations use the spectral slice filter in Fig. 8(d), the defocused multiplexer shown in Fig. 6(c) and for simplicity, all 16 R_n are unity with zero phase (i.e., the input OFC has a flat spectral intensity and phase). Figure 9(a) shows the static-OAWG case where the computed comb line modulations are static. Figure 9(a.1) shows that the waveform $a_k(t)$ is a repetitive waveform with a period equal to the OFC period, T. The spectrum of $a_k(t)$, Fig. 9(a.2), is obtained using a DFT and since the waveform is repetitive, $A_k(\omega)$ is a set of comb lines. The computed spectrum is spectrally sliced by the corrected slice filter [black and grey traces in Fig. 9(a.2)] and Fig. 9(a.3) presents the spectral modulations, $M_{k,n}(\omega)$, for the three center slices. Here, and as a general rule for the SS-OAWG algorithm, we actually use the corrected slice filter to spectrally slice $A_k(\omega)$ and therefore the calculated spectral modulations account for the shapes of both $S_n(\omega)$ and $H_n(\omega)$ in a single step. In the static-OAWG case [Fig. 9(a)], the corrected slice filters act as only isolation filters since the slice spectrum consists of just a single comb line. Figure 9(a.4) shows the temporal modulations [i.e., the IDFT of $M_{k,n}(\omega)$]. Since $a_k(t)$ is periodic, the modulations are static in time. Of course, previous static-OAWG theory produces the same set of modulations and does not require multiplication of $B(\omega)$ or application of the IDFT.

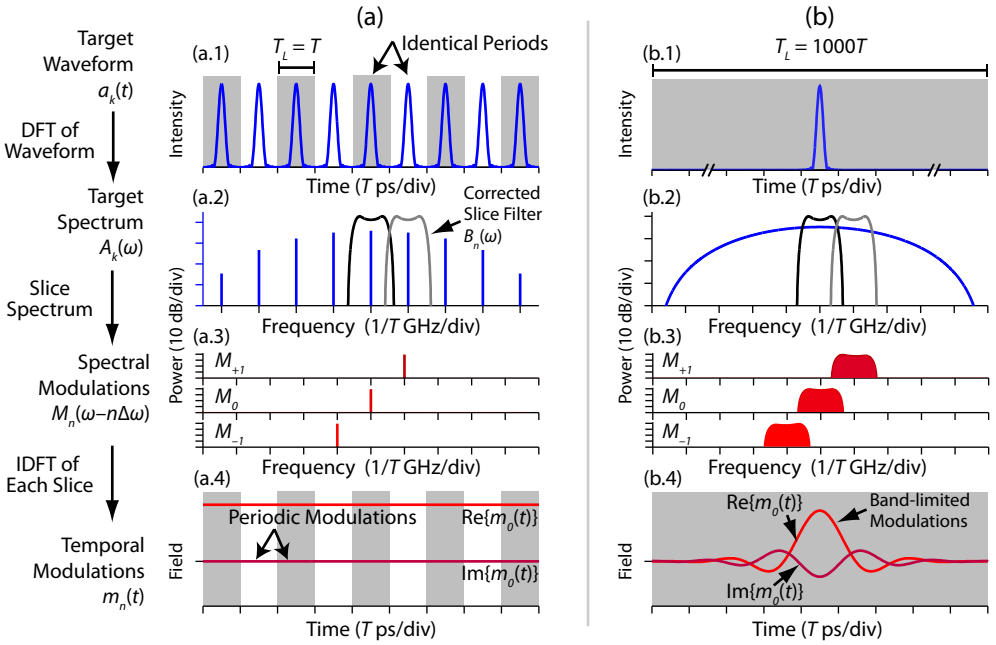

Fig. 9. Simulation example of the spectral-slice OAWG algorithm applied to a (a) periodic transform limited waveform, and (b) isolated transform limited waveform. (0.1) Temporal waveform. (0.2) Waveform spectral intensity. (0.3) Intensity of spectral modulations on three center comb lines. (0.4) Temporal modulations of the center comb line.

Figure 9(b) illustrates the SS-OAWG algorithm applied to a waveform with a duration much longer than the OFC period (e.g., $T_L > 1000T$—essentially infinite length). Figure 9(b.1)

#131467 - $15.00 USD Received 12 Jul 2010; revised 6 Aug 2010; accepted 7 Aug 2010; published 17 Aug 2010

shows the waveform when its intensity is non-zero and Fig. 9(b.2) presents its nearly continuous spectrum (i.e., an infinite length waveform implies a continuous spectrum). Applying the pre-emphasis filters to spectrally slice $A_k(\omega)$ yields the spectral modulations, $M_{k,n}(\omega)$. Figure 9(b.3) shows the spectral modulations for the three center slices which are bandlimited by the pre-emphasis filter. The temporal modulations of the central comb line, Fig. 9(b.4), are time-varying and when summed with the other modulations, accurately reconstruct the waveform.

The SS-OAWG algorithm flexibly generates many sets of modulations for a target waveform that are compatible with various gapless spectral multiplexers. However, the algorithm has a periodicity constraint. In theory, applying the SS-OAWG algorithm to a waveform with infinite duration removes the periodicity restriction. However, the latency is also infinite since the waveform must be specified a priori before performing the DFT.

5.3. The complete dynamic-OAWG algorithm and examples

The dynamic-OAWG algorithm uses both temporal slicing and the SS-OAWG algorithm to continuously generate spectral slice modulations capable of creating high-fidelity waveforms. Unlike the SS-OAWG algorithm, the modulations generated by the dynamic-OAWG algorithm must be optimized so that any distortions are minimized. Several examples will illustrate how the procedure works. For review, dynamic-OAWG first slices $a(t)$ into subwaveforms with duration T_L and a center-to-center spacing T_S using the temporal slice filter, $w(t)$, so that each subwaveform is given by $a_k(t) = a(t)w(t - kT_S)$. Then it computes the comb line modulations, $m_{k,n}(t)$, for each $a_k(t)$ using the SS-OAWG algorithm. Finally, for each comb line, it temporally stitches together the subwaveform modulations. Thus, the continuous modulations for each spectral slice are realized by

$$m_n(t) = \sum_{k=-\infty}^{+\infty} m_{k,n}(t)\,\mathrm{rect}\left[\left(t - kT_S\right)/T_L\right], \tag{6}$$

where rect is the rectangular function (i.e., normalized boxcar function where if $|t| \le ½$, then $\mathrm{rect}(t) = 1$, otherwise $\mathrm{rect}(t) = 0$). The rectangular function is included to emphasize that the modulations $m_{k,n}(t)$ produced by the SS-OAWG algorithm are repetitive with a period T_L and they are mathematically time gated when used in the dynamic-OAWG algorithm. The calculated $m_n(t)$ do not necessarily satisfy Eq. (3) since multiplication by the rect function in Eq. (6) occurs after $B_n(\omega)$ is applied to $M_{k,n}(\omega)$ and any new frequencies in $M_n(\omega)$ (e.g., from instantaneous jumps) are not included in the pre-emphasis (details in Section 5.4).

Figure 10 compares simulation results generated by the dynamic-OAWG algorithm for two different temporal slice filters. Figure 10(a) shows the rapid-update static-OAWG case where the rectangular temporal slice filter from Fig. 8(a), with T_S and T_L equal to the OFC period, is used on the long target waveform. (b) presents a more practical case where the overlapping temporal slice filter from Fig. 8(b), with $T_S = 2T$ and $T_L = 2T_S$, is used to temporally slice $a(t)$. In both cases, the multiplexer used to combine the spectral slices has the response shown in Fig. 8(d). The simulations show that the case (a) (i.e., rapid-update static-OAWG) requires extremely high-bandwidth modulation capability and spectrally flat multiplexers (e.g., star couplers) to avoid serious distortions. Alternatively, case (b) produces higher-fidelity waveforms while providing an optimization path for the dynamic-OAWG algorithm's parameters.

Figure 10(a.2) and 10(b.2) shows three subwaveforms that result when $w(t)$ is applied to $a(t)$. In case (a), the rectangular filter produces subwaveforms that are non-zero at their edges. Whereas case (b), the raised-cosine temporal slice filter, produces subwaveforms that overlap and also are zero at their edges. Figure 10(a.3) and 10(b.3) show some of the subwaveform modulations (real and imaginary values) calculated using the SS-OAWG algorithm after the rectangular function of Eq. (6) is applied. As mentioned previously, the DFT and IDFT in SS-OAWG algorithm require that both the subwaveforms and the modulations are periodic; the grey areas in Fig. 10(a.3) and 10(b.3) indicate one subwaveform period, T_L. In case (a), the subwaveform modulations are constant across each subwaveform [similar to Fig. 9(a.4)]. The

#131467 - $15.00 USD Received 12 Jul 2010; revised 6 Aug 2010; accepted 7 Aug 2010; published 17 Aug 2010

modulations are non-zero at the subwaveform edges, and therefore the rectangular gating function sets the modulations to zero.

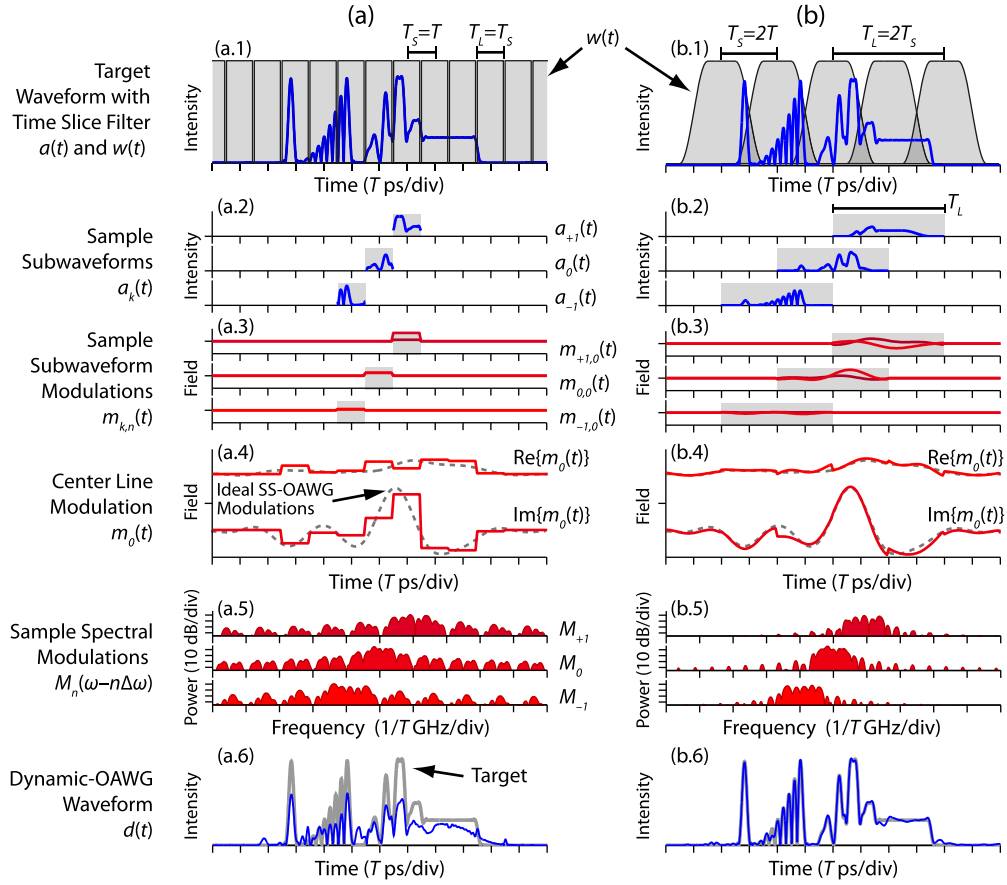

Fig. 10. Selected simulation results using the dynamic-OAWG algorithm for (a) rapid-update static-OAWG and (b) a more optimum case. (0.1) Target $a(t)$ and temporal slice filter $w(t)$. (0.2) Center three subwaveforms, $a_k(t)$. (0.3) Center line modulations, $m_{k,n}(t)$, for the three subwaveforms. (0.4) Center line modulation after summing all subwaveform modulations. (0.5) Spectral modulations (i.e., FT of temporal modulations). (0.6) Waveform $d(t)$ (blue) at the output of the multiplexer.

However for case (b), the longer temporal slices ($T_L = 4T$) and overlapping $w(t)$ drive the subwaveforms to zero at their edges. This produces much smoother $m_{k,n}(t)$ that also approach zero at their edges [similar to Fig. 9(b.4)]. Figure 10(a.4) and 10(b.4) show $m_0(t)$, the real and imaginary center line modulations calculated using Eq. (6) (solid) and the ideal spectral slice modulations (dashed) obtained by applying the SS-OAWG algorithm on $a(t)$ over a much longer window. For both cases, $m_0(t)$ has instantaneous jumps at the subwaveforms' edges (every T_S). However, for case (a), the jumps are much larger in magnitude and frequency while for case (b), $m_0(t)$ is nearly seamless. Figure 10(a.5) and 10(b.5) shows the Fourier transform of the three center-most comb line modulations. The modulations are not bandlimited although the modulations for case (b) occupy much less bandwidth than those of case (a). Figure 10(a.6) and 10(b.6) show the simulated dynamic-OAWG output waveform, $d(t)$, for the two cases. The output waveform in case (a) has greater than 10% normalized energy error (NEE) while case (b) has only 1% NEE where the normalized energy error is defined as

#131467 - $15.00 USD Received 12 Jul 2010; revised 6 Aug 2010; accepted 7 Aug 2010; published 17 Aug 2010

$$\mathrm{NEE} = \left[\int_{-\infty}^{+\infty} \left|\mu d(t) - a(t)\right|^2 \, dt\right]\left[\int_{-\infty}^{+\infty} \left|a(t)\right|^2 \, dt\right]^{-1} \tag{7}$$

where $d(t)$ is the generated waveform, $a(t)$ is the target waveform, and μ is a tuning parameter to minimize the NEE.

Review of the simulations indicate that case (b) produces a higher fidelity waveform since the required comb line modulations include some pre-emphasis and additionally are not spectrally truncated as severely by the multiplexer. As mentioned earlier, if the $m_{k,n}(t)$ are non-zero at the edges of the subwaveforms, then the gating in Eq. (6) introduces new frequencies that are not accounted for by the algorithm and distortions occur when the multiplexer filters these frequencies. That is, the modulations provided by the dynamic-OAWG algorithm only satisfy Eq. (3) for an all-pass multiplexer (i.e., no need for pre-emphasis). The distortions are difficult to quantify because they are both waveform and multiplexer dependent, and clustered near the edges of the subwaveforms. However, simulations show that the NEE is typically halved when T_S doubles. In an optimized design of $w(t)$ and $S_n(\omega)$, the dynamic-OAWG algorithm converges to the modulations determined using the spectral-slice OAWG of the infinite-length $a(t)$.

5.4. Optimization of the dynamic-OAWG algorithm

When using the dynamic-OAWG algorithm, there are many performance metrics that need simultaneous optimization or consideration: (1) waveform fidelity, (2) the minimum algorithm latency (i.e., how much of the waveform needs to be specified a priori), (3) pre-emphasis loss for certain filter shapes, (4) bandwidth efficiency, and (5) computational redundancy. Figure 11 depicts the waveform fidelity (expressed as NEE) versus latency for the two types of temporal slice filters: the non-overlapping rectangular filter and the overlapping filter. Since fidelity is waveform and multiplexer dependent, the simulations take the average fidelity of a set of 100 random waveforms that each have flat spectral intensity and uniformly distributed random spectral phase ($-\pi$ to $+\pi$ rad). This produces a noise-like flat intensity waveform spread across the entire period. For each $w(t)$, the waveform fidelity is compared for four different corrected slice filters [see Fig. 11(c)] to understand how they impact fidelity and latency. In general, waveform errors occur at the edges of each temporal subwaveform because this is where the instantaneous jumps in the modulations occur and are filtered. The fidelity is improved by increasing T_S or T_L, optimizing $S_n(\omega)$ to generate a flatter corrected slice filter with smooth roll-off, $B_n(\omega)$, optimizing the multiplexer for greater spectral overlap, and forcing the time slice filters to slowly roll-off to zero at their edges.

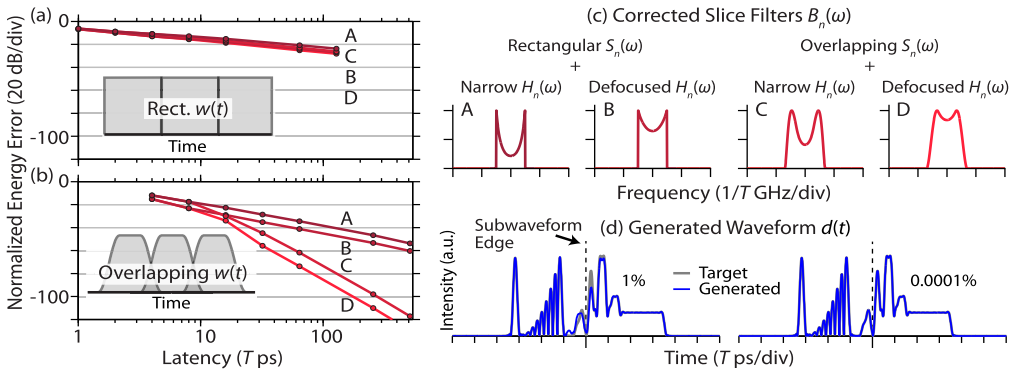

Fig. 11. Optimization of the dynamic-OAWG algorithm for waveform fidelity and latency. (a,b) Error energy for (a) a rectangular $w(t)$ and (b) an overlapping $w(t)$ in conjunction with the (c) corrected slice filters A, B, C, and D. (d) Comparison of the target and generated waveforms with 1% error (–20 dB) and 0.0001% error (–60 dB).

#131467 - $15.00 USD Received 12 Jul 2010; revised 6 Aug 2010; accepted 7 Aug 2010; published 17 Aug 2010

For the rectangular $w(t)$ cases in Fig. 11(a), the NEE drops by half (−3 dB) when the latency doubles. This is because the combined modulations have significant energy at the subwaveform edges. In turn, the subwaveform modulations are large and produce discontinuities when combined together. These discontinuities are filtered and create distortions located near the subwaveform window edges. The corrected slice filter does not accommodate these new frequencies and the improvement in fidelity versus latency is mainly the result of fewer distortions or glitches across the waveform.

In Fig. 11(b) the NEE decreases much faster as a function of latency. This is due to the use of the overlapping $w(t)$ that forces the subwaveforms to zero at their edges and therefore the corresponding subwaveform modulations approach zero at their edges. Here, optimizing the impulse response of the corrected slice filter plays a strong role in reducing the waveform errors. Generally, corrected slice filters that have wider bandwidths and roll off smoothly have impulse responses that are more localized in time.

Figure 11(d) illustrates two waveforms with different fidelity. The left waveform uses the β = 1/2 temporal slice filter and corrected slice filter C. The right waveform uses the rect temporal slice filter and corrected slice filter C. Waveforms are computed at 60T ps latency. The left waveform has 1% NEE and there is a noticeable difference between the generated waveform $d(t)$ and the target waveform $a(t)$. The most significant errors are localized near the subwaveform transition points. The right waveform has only 0.0001% NEE and it is indistinguishable from the target on the scale shown.

6. Dynamic-OAWG and an analogy with OAWM

A significant insight into the field of optical arbitrary waveform generation and measurement is possible once one realizes that OAWG is analogous to OAWM. Referring to Fig. 12, the spectral demultiplexer isolates each comb line of an input OFC to a separate waveguide. Then four-quadrature modulations (e.g., *I/Q* modulation), determined with DSP pre-processing, are applied to each OFC comb line in a parallel manner. The spectrally broadened comb lines are coherently combined using a multiplexer with spectrally overlapping adjacent passbands, producing the arbitrary optical waveform. The spectrum of the resulting waveform is continuous with the phase and amplitude fully specified across the entire bandwidth. If the modulation is continuously applied, the waveform's temporal length can be infinite.

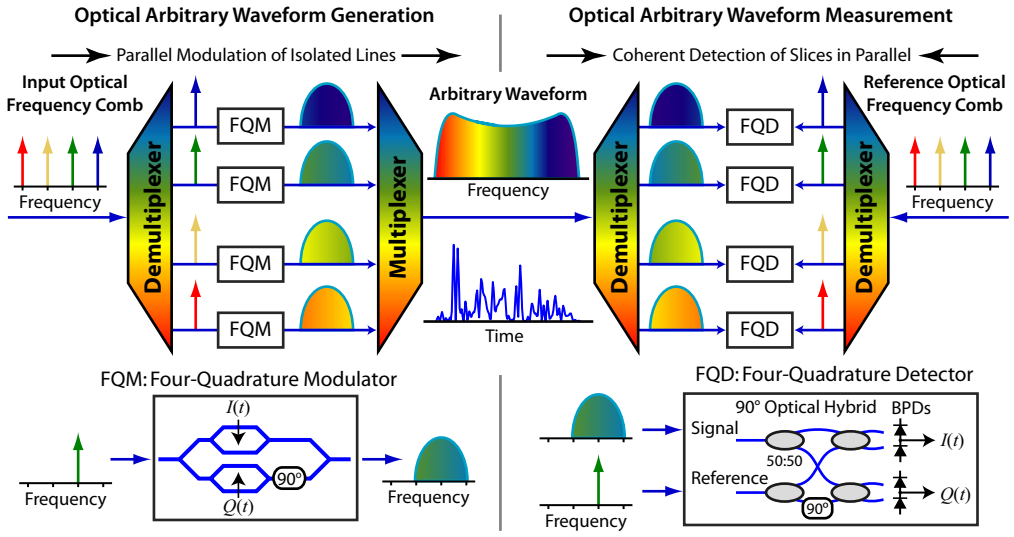

Fig. 12. An illustration showing the OAWG and OAWM analogy. BPD: balanced photodiodes.

OAWM is essentially the inverse of OAWG—instead of producing a waveform by creating and combining spectral slices, we are splitting the arbitrary waveform and coherently

#131467 - $15.00 USD Received 12 Jul 2010; revised 6 Aug 2010; accepted 7 Aug 2010; published 17 Aug 2010

measuring the spectral slices. Looking at the right half of Fig. 12, the arbitrary waveform is spectrally sliced by a gapless demultiplexer. On the far right, each line of a reference OFC is isolated by a spectral demultiplexer to a separate waveguide. Then, these two signals become the inputs to an array of coherent four-quadrature detectors (i.e., optical digital coherent receivers). After removing the effects of optical and electrical filters in the measurement system (e.g., demultiplexer transmission, photoreceiver response, etc.), the signal waveform is reconstructed from the individual slice *I/Q* signals using DSP. If the data is recorded continuously, the spectral resolution is limited only by the reference OFC stability and digital coherent receiver performance.

A detailed description and demonstration of the OAWM technique is presented in [8]. The work shows that parallel coherent detection of spectral slices from an arbitrary optical waveform enables scalable measurement bandwidth without increasing the required electrical bandwidth. The demonstration includes real-time, full-field optical waveform measurements with an instantaneous bandwidth of greater than 160 GHz and record lengths of 2 μs (i.e., 500 kHz spectral resolution). Thus, OAWM is a corroboration of continuous and dynamic OAWG techniques.

7. Conclusion

This paper described dynamic-OAWG and OAWM techniques that provide for high-fidelity continuous optical waveform generation and measurement in a bandwidth scalable fashion. The generation technique overcomes waveform fidelity limitations associated with rapid-update static-OAWG by using a temporal/spectral domain algorithm to calculate the comb line modulations that are compatible with spectral multiplexers and a waveform shaper design that incorporates quadrature modulation and gapless spectral multiplexers. Simulations showed how to create high-fidelity waveforms by optimizing both the spectral multiplexer passband shape and the temporal and spectral slicing choices within the dynamic-OAWG algorithm. This work enables future demonstrations of dynamic-OAWG that use an integrated-optic platform [12] to ensure stability between the spectral slices while also providing a simple way to scale the number of spectral slices and to incorporate large arrays of modulators.

Since both dynamic-OAWG and OAWM are bandwidth scalable and capable of continuous operation, their achievable spectral and temporal resolutions are not fundamentally limited. It is the stability of the OFC, and technological issues associated with large-scale device integration, that will likely determine the ultimate performance of a combined system.

Acknowledgments

This work was supported in part by the Defense Advanced Research Projects Agency (DARPA) and the Space and Naval Warfare Systems Command (SPAWAR) under OAWG contract HR0011–05–C–0155.

#131467 - $15.00 USD Received 12 Jul 2010; revised 6 Aug 2010; accepted 7 Aug 2010; published 17 Aug 2010